THE SNS LASER STRIPPING EXPERIMENT AND ITS IMPLICATIONS ON BEAM ACCUMULATION

S. Cousineau, A. Aleksandrov, T. Gorlov, Y. Liu, A. Menshov,
M. Plum, A. Rakhman, ORNL, TN 37922, USA
D. Johnson, Fermilab, Batavia, IL 60510, USA

Abstract

The laser assisted H^- charge exchange concept is under development at the SNS as on option for replacing traditional carbon-based foil technology in future HEP accelerators. A laser based stripping system has the potential to alleviate limiting issues with foil technology, specifically radiation from beam scattering and foil survivability, paving the way for accumulation of higher density proton beams. This paper discusses the advantages and limitations of a laser-based stripping system compared with traditional foil-based charge exchange systems for various beam accumulation scenarios, scaling from SNS experience with high power beam injection and calculations of laser stripping parameters. In addition, preparations for an experimental demonstration of laser assisted stripping for microsecond long 1 GeV, H^- beams are described.

INTRODUCTION

The standard method for accumulating intense beams of protons is through H^- charge exchange from a linac into a synchrotron. In this scheme, an H^- beam from a linear accelerator is merged with a circulating proton beam in a ring. The merged beam is subsequently passed through a thin (~μm) carbon foil that strips the electrons from the H^- ions to yield a proton beam [1]. While in principle this non-Liousvillian technique can yield indefinitely dense proton beams, in practice the beam density is limited by the stripping mechanism.

The presence of the foil in the beamline introduces two major performance limitations. First, energy deposition in the foil leads to foil heating. Foils suffer vulnerabilities in their structural integrity when thermal effects are high causing warps, holes and tears. The primary failure mechanism for foils is sublimation above a certain temperature threshold, which translates into constraints on the achievable beam power densities. Existing high power machines such as the SNS accelerator are already estimated to operate just below this limit [2]. Second, particle scattering in the foil leads to large levels of beam loss and activation. This issue is pervasive across machines that utilize H^- charge exchange injection, and results in residual radiation levels typically an order of magnitude greater than the rest of the accelerator [3].

While schemes such as injection painting can be used to minimize beam foil trav0ersals and their subsequent effects, they are not infinitely scalable because they result in progressively larger beam emittances and machine apertures. An interesting question to consider is what a proton accumulation scenario would look like if the charge exchange process could be accomplished without the use of a foil. This paper will explore this question through a set of experiments in the SNS proton accumulator ring. Following this, the development of laser stripping method, a foil-free alternative stripping scheme, will be described.

HIGH DENSITY EXPERIMENT AT SNS

Experimental Configuration

The SNS accumulator ring accumulates up to 1.5e14, 1 GeV protons during a 1 ms, 1000 turn accumulation cycle. The injection process utilizes 400 μg/cm2 nanocrystalline diamond foils. Correlated dual plane injection painting is employed via a set of injection kickers which fall off by 52% over 1000 turns in a $\sqrt{turns}$ fashion.

The purpose of the experiment was to approximate what beam parameters could be accomplished in the absence of injection foil limitations. While the injection foil can not in reality be removed from the system, the beam can be run in a configuration with reduced repetition rate, i.e., 1 Hz instead of the 60 Hz, to avoid foil heating and allow for temporarily higher levels of beam loss. Besides the repetition rate, the remainder of the beam parameters were fixed at nominal production values, with 1.43e14 ppp accumulating over 1000 turns. This produces a "1.4 MW equivalent" beam in a per pulse sense.

The effects of three injection painting scenarios were explored: 1) No painting, 2) Nominal painting, and 3) Shallow painting with an injection kicker amplitude fall of 30% (compared with the nominal 52%). For each of these scenarios, the initial injection kicker amplitudes were varied to alter the beam emittance, up until the point where injection losses exceeded acceptable values even at 1 Hz. For each setting, the beam loss in the ring and the final beam emittance was recorded. Due to constraints on the allowable peak beam density on target, the emittances were only measured directly for the nominal production configuration. The remainder of the emittances were derived from ratios of the rms beam sizes with the production case at a common wirescanner location.

Results

Fig. 1 shows the results of the measured emittances for the various beam configurations. The upper right point, with emittance (ε_x=29 mm*mrad, ε_y=36 mm*mrad), represent the nominal configuration. By contrast, the smallest emittance achieved was (ε_x=12 mm*mrad, ε_y=17 mm*mrad), roughly a factor of two smaller in each plane.

ISBN 978-3-95450-174-8

Figure 2 shows the horizontal profiles for the nominal case compared with the smallest emittance case. No visible tails were seen on the smaller emittance case, and no space charge limitations were encountered.

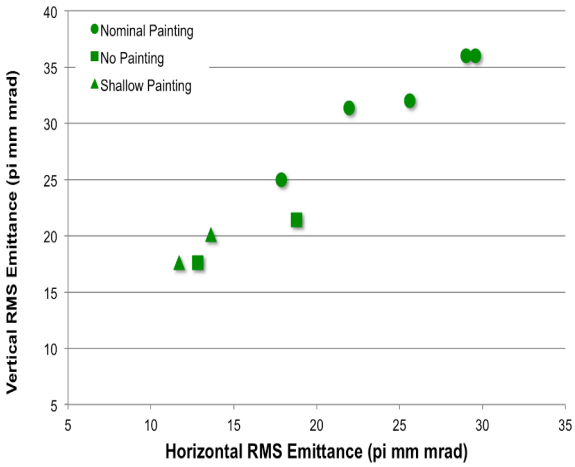

Figure 1: Measured horizontal and vertical rms emittances.

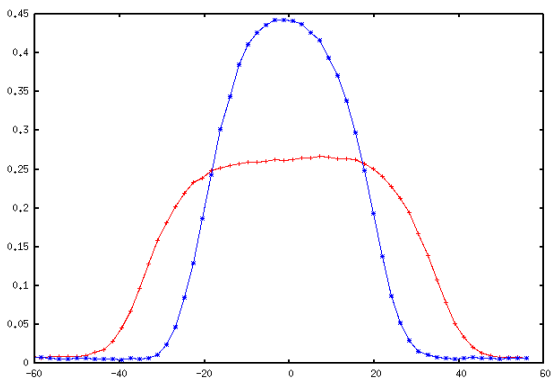

Figure 2: Horizontal beam profiles after extraction from the ring for the upper right most data point on Fig. 1 (red), and the lower leftmost data point on Fig. 1 (blue).

The lower bound on beam emittance in the experiment was set by the injected beam loss. Fig. 3 shows the beam loss monitor (BLM) signal for one of the main injection area BLMs, versus measured beam emittance for the various accumulation scenarios. As seen, a factor of two decrease in emittance resulted in a factor of ten increase in injected beam loss. Even with the reduced repetition rate, it was considered hazardous to the injection foil to decrease the emittance beyond this point.

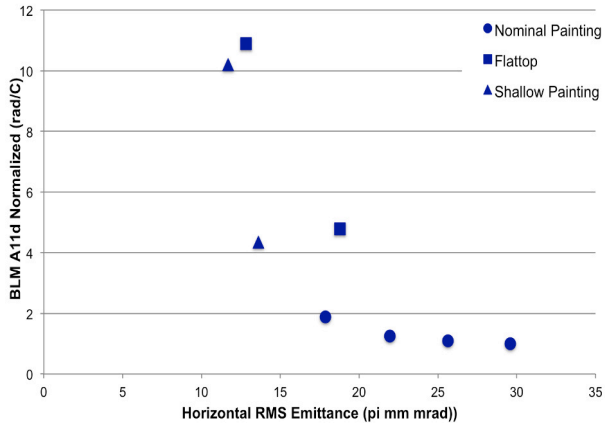

Figure 3: Injection BLM reading versus measured horizontal emittance.

Discussion of Results

It is interesting to consider the implications of the lowest emittance case, by scaling the current SNS full-power parameters with these numbers for scenarios (a) with an injection foil, and (b) without an injection foil.

Case (a): The current residual radiation values in the SNS injection region are about 0.8 – 1 rem/hr at 30 cm. The observed factor of ten increase in beam loss, corresponding to the smallest emittance beam, would result in roughly 10 rem/hr of radiation in this region. This would have severe implications on routine maintenance of the injection foil system components. In addition, from simulations, the estimated foil temperatures for the nominal 1.4 MW operation peak at about 1550 K, which is just below the predicted sublimation range of 1575 K-2270 K [2]. The thermal power radiated scales as temperature to the fourth power, and thus a factor of ten increase in radiation would result in foil temperatures in the neighbourhood of 2700 K. At these temperatures, the foils would sublimate within minutes when operating at the full repetition rate of 60 Hz.

Case (b): Without the injection foil present, neither the issue of foil sublimation nor the issue of activation from foil scattering would exist. Radiation levels in the injection region would be reduced to the nominal SNS ring levels of < 5 mrem/hr. Furthermore, operation with a factor of two smaller in beam emittance would translate in to a factor of $\sqrt{2}$ reduction beam pipe aperture. For instance, in principal the nominal SNS ring aperture could have been reduced from 100 mm to 70 mm, which would have saved in fabrication costs and vacuum requirements. Finally, the current painting scheme, which is designed to minimize circulating beam foil traversals, could be optimized for other purposes, such as mitigating space charge effects.

ISBN 978-3-95450-174-8

LASER ASSISTED STRIPPING

The Laser Stripping Concept

An alternative approach to foil based charge exchange injection is laser-assisted H^- stripping. In this concept, an H^- ion beam is passed through a dipole magnet which strips off the first electron through the process of Lorentz stripping (H^- to H^0). The second, inner electron is too tightly bound to be stripped off using a conventional magnet while in the ground state, and thus a laser is used to excite the electron to a higher quantum state with a smaller binding energy (H^0 to H^{0*}). While in the excited state, the H^{0*} is passed through a second dipole magnet of comparable strength to the first, which strips off the remaining electron to produce a proton (H^{0*} to p). Due to the absence of material in the path of the beam, this technique does not suffer from the same performance limitations as foil-based charge exchange injection, and is scalable to infinitely high beam densities.

Though the idea of laser stripping was conceptualized over three decades ago [4], the technique was limited by the Doppler broadening of the resonant excitation frequency of the laser, and available laser technology. This limitation was overcome in a 2006 proof of principle experiment which utilized a diverging laser beam to introduce a frequency sweep in the rest frame of the laser. The experiment demonstrated successful (>90%) stripping of a 6 ns, 1 GeV H^- beam using a 10 MW UV laser [5]. Unfortunately, a direct scaling of this experiment to full duty factors results in unrealistically large laser powers. To advance this concept one must find ways to reduce the laser power requirement to achievable levels.

The 10 μs Laser Stripping Experiment

The next step in the development of the laser stripping method is a demonstration of stripping for a 10 μs beam. This is a factor of one thousand improvement over the initial demonstration of the concept. The experiment will take place in the SNS High Energy Beam Transport line (HEBT) which connects the superconducting linac (SCL) to the ring, and will rely on the successful implementation of a number of laser power savings techniques [6].

Laser Power Savings Techniques The laser power savings techniques can be broken down into to categories: 1) Methods for reducing the required peak power, and 2) Methods for reducing the required average power.

To reduce the require laser peak power, one must overcome the problem of the resonant frequency spread without using a diverging laser beam, which reduces the laser light density and therefore requires more peak power. The required laser frequency for resonant excitation of an H^0 particle depends on the particle's energy and the angle between the particle and laser beam trajectory. The dispersion function, which relates a particle's energy with its trajectory, can be tailored to manipulate the individual angles such that each energy and angle pair yields the same resonant excitation frequency [7]. Once the dispersion tailoring is accomplishment, the remaining energy spread is due to transverse divergence of the beam and can be minimized by requiring that Twiss α=0. Finally, in order to maximize the interaction between the laser and ion beam, the vertical beam size should be minimized at the interaction point. The dispersion and Twiss parameters are accomplished through tuning of quadrupoles upstream of the experiment, and have been demonstrated simultaneous in a repeatable fashion. Taken together, these methods result in a factor of ten reduction in the required UV laser peak power, from 10 MW to 1 MW.

The average required laser power can be computed through the following equation:

$$P_{average} = P_{peak}(\sigma_v, \Delta f_{resonant}) \times (\sigma_l \; f_{micro} \; f_{macro}) \times \Delta t$$

The 1 ms SNS macropulse is composed of a 402.5 MHz train of ~50 ps micropulses. Thus for the majority of the time there is no ion beam present for the laser to interact with, and a significant reduction in average laser power can be realized by temporal matching the pulse structure of the laser beam with the ion beam. Fig. 2 shows the configuration of the laser pulse and the resulting 402.5 MHz, 50 ps micropulses. The laser is a master oscillator power amplification (MOPA) scheme with 402.5 MHz, ~50 ps pulses generated from a 1064 nm seed laser and passed into a pulse picker to create 10 μs macropulse bursts. The light is then amplified in three stages before a two-stage harmonic conversion to the required 355 nm wavelength. This laser has been measured to produce 1 – 3 MW peak power, for 30 – 55 ps bursts.

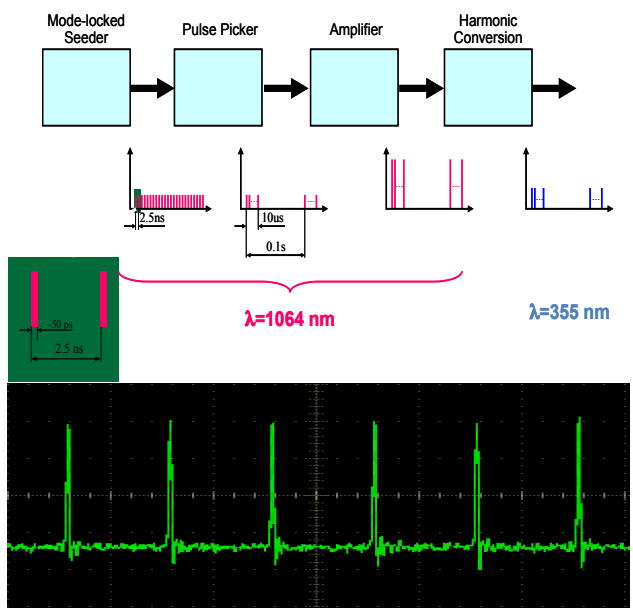

Figure 4: (Top) Schematic of the MOPA configuration for the high power UV laser beam. (Bottom) Meausred 402.5 MHz, 50 ps UV laser pulses.

ISBN 978-3-95450-174-8

The final savings on average laser power comes from a longitudinal squeeze of the ion beam to produce full overlap with the laser beam pulse. Nominally, the ion beam expands under the influence of space charge and momentum spread after exiting the last accelerating cavity. For the laser stripping experiment, however, the last ten superconducting cavities are configured to provide a longitudinal waist in the beam at the downstream interaction point for the experiment. This technique has been successfully demonstrated several times.

Putting together all of the power savings techniques, the final average laser power is ~2 W, which is sufficient for the 10 μs stripping experiment, including some margin.

Experimental Configuration The interaction point for the laser stripping experiment will be located in the SNS HEBT, in a low radiation region downstream of the ninety degree achromat. This location takes advantage of the bend for dispersion tailoring and has the upstream optics necessary to achieve all of the required Twiss parameters. The designed and as-installed experimental vessel for the interaction point is shown in Fig. 3 below. The vessel contains two ~ 1 T permanent dipole magnets mounted on a retractable actuator, a dual plane wirescanner to confirm the transverse beam parameters at the interaction point, a downstream BCM for validating the experiment, and input an exit windows for the laser as well as two viewports.

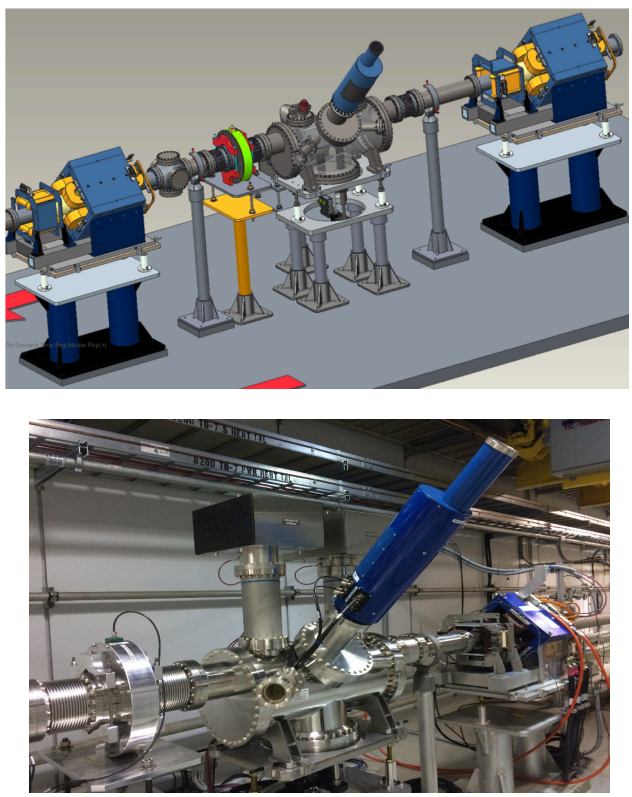

Figure 5: (Top) Engineering drawing of the laser stripping experimental vessel. (Bottom) Photo of the as-installed vessel.

In order to protect the laser and provide flexibility in the experimental schedule, the high power UV laser will be located in the ring service building and transported 70 m to a local optical table adjacent to the interaction point. Two major concerns with remote placement of the laser were power loss in transport and pointing stability.

The power losses on the mirrors and windows were independently measured, and the total path length in air was simulated by cycling the laser through six iterations of an 8 m, four-mirror loop. The results are promising: The power loss per mirror was less than 1%, and the power loss in air, extrapolated to 70 m, was less than one third. The major source of the power loss in air is believed to be Fresnel diffraction at the aperture and loss of higher order modes in transport, an effect which diminishes with distance. Furthermore, it was determined that a single piezo-electric transducer (PZT) would be sufficient to provide laser pointing stability.

Taking into account the estimated power loss in transport, and inputting the experimentally-measured ion and laser beam parameters into the pyORBIT model of the stripping system [8], the final laser stripping efficiency is estimated to be >90%. The installation for the experiment is nearly complete and the demonstration of 10 μs stripping is expected to commence in Spring 2016.

Laser Power Recycling and 1 ms Stripping

To extend the laser stripping concept beyond microsecond pulse lengths and into operational parameter regimes, one must find a way to extend the high power laser pulse without exceeding commercially available average UV laser powers in the range of 1-10 W. Since only one in 10^7 photos is "spent" during each passage of the laser beam through the ion beam, a logical option is to recycle the laser pulses. Optical power recycling cavities provide power enhancement through the process of coherent addition, allowing lasers of arbitrary burst lengths to be amplified to high peak powers. As such, for a constant input laser power, one can utilize a longer duration pulse with a lower peak power, and subsequently amplify to high peak power in the cavity.

After the 10 μs demonstration, the next step in the laser stripping development will be to employ such a power recycling cavity to demonstrate 1 ms capable laser stripping of the SNS 1 GeV H^- beam. The current experimental vessel, shown in Fig. 5, was designed to accommodate the recycling cavity with only minor modification. In addition, a doubly resonant power enhancement cavity scheme was has been under development to realize amplification of burst mode UV laser pulses. In the most current version of the concept, an auxiliary IR laser beam is used to lock the cavity and provide stable amplification of the UV laser macrobursts through a frequency tuning approach [9]. The scheme resulted in a factor of 50 enhancement of a lower power UV beam, exceeding the initial proposal goal by almost a factor of two. However, at this stage the peak in cavity power is limited to 120 kW, solely by the cavity mirror

ISBN 978-3-95450-174-8

damage threshold. Modifications to the system to overcome this limitation have been identified and will be implemented in the near future.

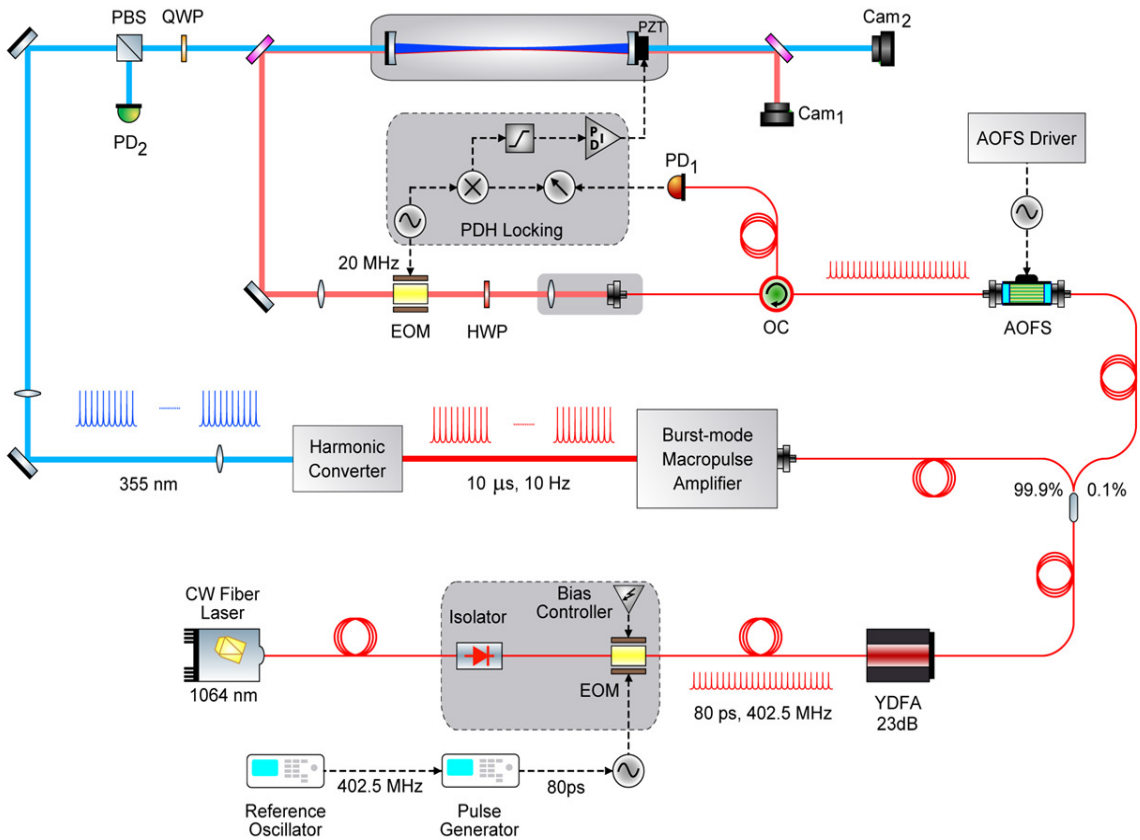

Figure 6: Schematic of the doubly resonant power recycling cavity for amplification of burst mode UV laser pulses.

ACKNOWLEDGMENT

This work has been partially supported by U.S. DOE grant DE-FG02-13ER41967. Oak Ridge National Laboratory is managed by UT-Battelle, LLC, under contract DE-AC05-00OR22725 for the U.S. Department of Energy.

REFERENCES

[1] S.Y Lee, Accelerator Physics, World Scientific, 1998.

[2] Michael Plum, Jeffrey A Holmes, R.W. Shaw, and C.S. Feigerle, "SNS Stripper foil development program," Nuclear Instruments and Methods in Physics Research A, vol. 590, pp. 43-46, 2008.

[3] Sarah Cousineau, "High Power Proton Beam Facilities: Operational Experience, Challenges, and the Future ," in International Particle Accelerator Conference 2015, Richmond, 2015, pp. 4102-4106.

[4] A. Zelensky, S.A. Kokohanovskiy, V.M. Lobashev, N.M. Sobolevskiy, and E.A. Volferts, Nuclear Instruments and Methods Phys. Res., Sect. A, vol. 227, no. 429, 1984.

[5] V. Danilov et al., "Proof-of-principle demonstration of high efficiency laser-assisted H- beam conversion to protons," PRST-AB, vol. 10, no. 053501, 2007.

[6] Sarah Cousineau, "Status of Preparations for a 10 microsend laser-assisted H0 beam stripping experiment," in International Particle Accelerator Conference 2014, Dresden, pp. 1864-1866.

[7] V. Danilov, "Future prospects for laser stripping injection in high intensity machine," in *Proceedings of the ICFA 2008 Workshop on High Brightness Hadron Beams*, Nashville, 2008, pp. 284-289.

[8] T. Gorlov, V. Danilov, and A. Shishlo, "Laser-assisted H- charge exchange injection in mangetic fields," *PRST-AB*, vol. 13, no. 050101, 2010.

[9] Abdurahim Rakhman, Yun Liu, Chunning Huang, and Mark Notcutt, "Doubly-resonant Fabry0Pero cavity for power enhancement of burst-mode picosecond ultraviolet pulses," in CLEO, San Jose, 2015.

ISBN 978-3-95450-174-8